Available online at www.sciencedirect.com
SCIENCE DIRECT®
ELSEVIER
Ultramicroscopy 100 (2004) 413–419
ultramicroscopy
www.elsevier.com/locate/ultramic

Applications of field-enhanced near-field optical microscopy

A. Bouhelier*, M.R. Beversluis, L. Novotny

The Institute of Optics, University of Rochester, Rochester, NY 14627, USA

Received 4 June 2003; received in revised form 22 October 2003; accepted 30 October 2003

Abstract

Metal nanostructures such as sharp tips can enhance emission yields through shape-induced local field enhancement. The enhancement originates from two mechanisms: surface plasmons and electrostatic lightening rod effects. We present fluorescence imaging using the strong local field created at the apex of a gold tip and demonstrate optical resolution of 25 nm. The enhancement effect gives also rise to photoemission from the tip itself. Measured spectra of the tip emission show a broad band continuum together with a second-harmonic peak. Both continuum and second-harmonic are confined at the apex of the tip. We find that, depending on the spectral position, the photoluminescence originates either from intraband or from interband transitions. The nonlinear response can be described by a single dipole oscillating at the second-harmonic frequency and oriented along the tip axis. These unique properties can be used to map focal fields distributions.

Keywords: Near-field optics; Field enhancement; Second-harmonic generation; Photoluminescence

1. Introduction

Metallic nanostructures are successfully used to increase the yield of particularly small scattering and fluorescence cross-sections. A well-known effect is the local enhancement of Raman cross-sections induced by the roughness of a thin metallic film or by metal nanostructures [1,2]. Local resonances of the surface topology are believed to be responsible for the field enhancement effect [3]. While resonances are generally spatially randomly distributed on metallic films [4], they can be localized at the apex of a sharp metallic tip [5]. The enhancement at such a structure arises from a combination of an electrostatic rod effect and surface plasmon oscillations. The electrostatic rod effect, determined by the geometric singularity of the tip apex, is highly sensitive to the excitation polarization. It is excited only when the polarization of the incident source is aligned with the tip axis [6,7]. On the other hand, surface plasmons represent a collective electron oscillation on the surface of the structure, and have well-defined resonances that are sensitive to both wavelength and polarization of the excitation source. For an extended conical geometry such as a tip, the conditions leading to a surface plasmon resonance are not obvious and will be strongly influenced by small variations in the tip shape. The electrostatic enhancement, however, seems more

*Corresponding author. Present address: Argonne National Laboratory, Chemistry Division & Center for Nanoscale Materials, Building 200, 9700 S. Cass Avenue, Argonne, IL 60439, USA. Tel.: +1-630-252-5796.

E-mail address: bouhelier@anl.gov (A. Bouhelier).

0304-3991/$ - see front matter © 2004 Elsevier B.V. All rights reserved.
doi:10.1016/j.ultramic.2003.10.007

controllable since it relies mainly on a suitable polarization. A common technique to provide such a polarization is to excite the tip with a laser beam incident on the side of the tip and polarized along the tip axis [8]. An alternative method is to use longitudinal fields created in the focal region of a highly focused laser beam [9]. These longitudinal fields point in direction of light propagation and provide the necessary on-axis polarization conditions.

The enhanced field near the apex of a gold tip constitutes a nanoscale light source whose size is determined by the sharpness of the tip. This light source can be used for local spectroscopy and high-resolution near-field optical imaging. The spatial resolution achievable with this technique is only determined by the tip size, and the signal to noise is defined by the strength of the field enhancement effect. In the following experiments, field enhancement at the apex of a sharp gold tip is generated by the longitudinal fields of a focused Gaussian beam. We use a laser providing femtosecond pulses with high peak intensity in order to excite fluorescence from *J*-aggregates by a 2-photon absorption process [10]. We find that the fluorescence emission competes with a background emission from the tip itself. This background is due to second-harmonic generation and broadband photoluminescence from the tip material. Both, second-harmonic and continuum generation are the result of the complex interplay between the tip material and the local field enhancement effect.

2. Description of the apparatus

A schematic of our experimental setup is depicted in Fig. 1. A tip is excited by a mode-locked Ti:sapphire laser producing 120 fs pulses at a wavelength of 780 nm. The laser beam is spatially filtered using a 10 μm pinhole to produce a Gaussian beam profile. Before entering the microscope, the excitation light is filtered using a 20 nm band pass filter to remove all visible and infrared laser fluorescence. The beam is expanded to overfill the back aperture of a high numerical aperture objective (NA = 1.3). The objective is focused on a glass cover slip. Electrochemically etched gold tips are positioned to a few nanometer above a glass substrate by means of shear-force regulation [11]. The tip can be moved laterally with a piezo-electric ceramic tube into a region of strong longitudinal field. The optical response of sample and tip is collected by the same objective. The light is then either directed to a sensitive avalanche photodiode (APD) or to a spectrograph for measuring emission spectra. In combination with the APD, we used dielectric bandpass filters transmitting between 500 and 700 nm and providing more than 12 optical density (OD) of attenuation outside of this band. For the spectrograph, a 4-f relay system was used in combination with two 780 nm notch filters.

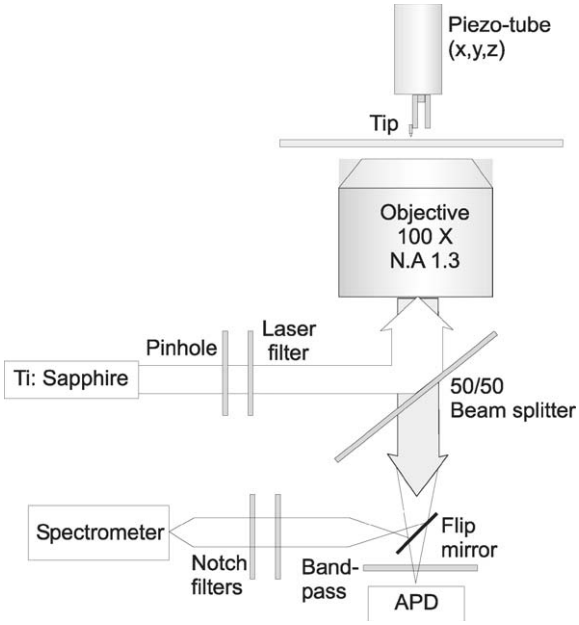

Fig. 1. Experimental set-up. A Ti:sapphire laser is spatially and spectrally filtered and focused on a glass cover slip. A gold tip is held above the focal spot. The emission of the sample, respectively of the tip, is collected by the same objective and is focused on either an avalanche photodiode (APD) or a spectrometer.

3. Near-field 2-photon excitation of *J*-aggregates

Pseudo-isocyanine (PIC) *J*-aggregates were chosen to demonstrate high-resolution optical imaging

and spectroscopy. *J*-aggregates consist of a nanometric ribbon of PIC dye molecules incorporated into a polymer [12]. The fluorescence of the PIC exhibits a sharp absorption peak characteristic of a delocalized excitation state. A high concentration of dye molecules combined with a distinct topographical signature make it an ideal test sample for near-field optical imaging. The high peak power associated with the ultra-short laser pulses allows the excitation of the *J*-aggregates via a two-photon absorption process. This has two distinct advantages: first, the large spectral separation between the excitation (780 nm) and the emission (500–700 nm) allows for efficient background suppression. Second, due to the nonlinear character of the two-photon absorption, the fluorescence emission scales with the square of the enhancement factor, providing a higher signal-to-noise ratio as compared to one-photon excitation [10].

J-aggregates are prepared following the method described in Ref. [12]. A droplet of the solution was spun onto a clean glass cover slip, then placed on our microscope. A sharp gold tip was positioned a few nanometer above the focal spot of a Gaussian beam. The tip was aligned with the longitudinal field in order to create strong field enhancement. The sample was laterally raster scanned underneath the tip. The emission of *J*-aggregates was recorded for each tip position, allowing us to construct a fluorescent image of the sample as seen in Fig. 2(a). The simultaneously acquired topographic image is displayed in Fig. 2(b). The topography confirms the ribbon-like structure of the *J*-aggregates, which forms a mesh of interwoven strands. The aggregates have a variety of sizes ranging from a few nanometers to several tens of nanometers. The fluorescence image essentially reproduces the pattern seen in the topographic image with the advantage of providing an emission spectrum for each pixel of the image. The estimated optical resolution is 25 nm, demonstrating thus the high resolution capability of the technique. The near-field nature of the excitation source is readily seen when the distance between the tip and the sample is varied as seen in Fig. 3. A constant background representing the far field contribution dominates the signal when the tip is retracted. A steep increase of the fluorescence

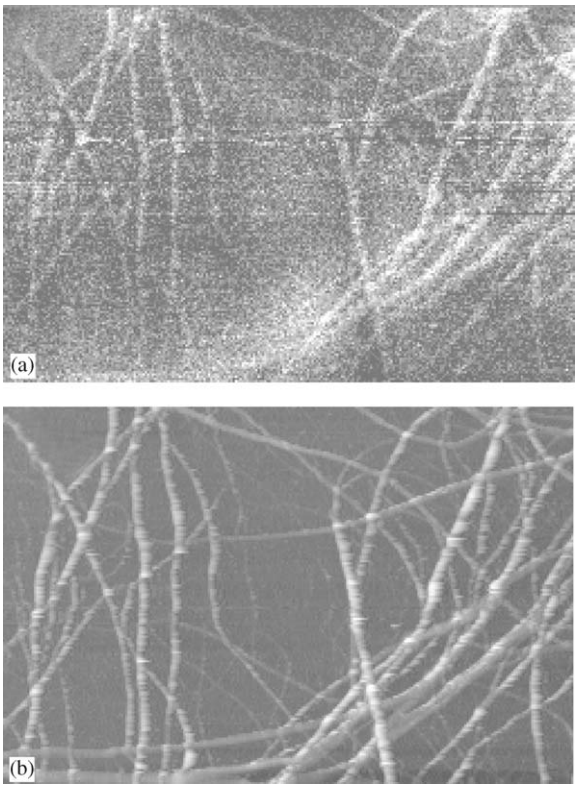

Fig. 2. (a) Fluorescent emission image of *J*-aggregates. The optical resolution is $\sim$25 nm. (b) Topographical image. The aggregates form an interwoven mesh of tubulus. Images are 3 μm × 2 μm.

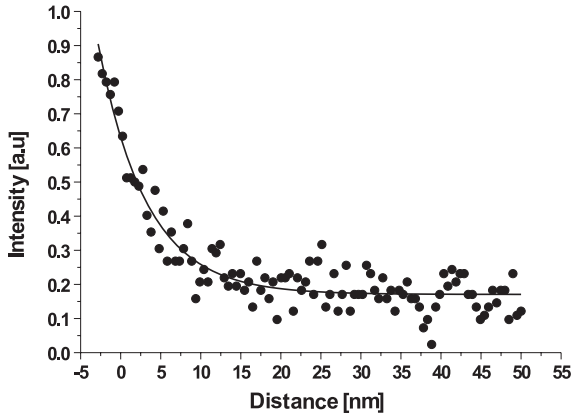

Fig. 3. Tip–sample distance dependence of the fluorescent emission. The experimental data (circles) can be fitted with a single exponential with a decay constant of approximatively 6 nm (solid curve).

signal is detected when the tip approaches the last 10 nm. The fluorescent rate can be fitted by a single exponential decay with a typical length of ~ 6 nm. We observed similar dependence if the tip is retracted from the aggregates (data not shown). It is worth noticing that fluorescence quenching by the metal tip does not play an important role. The *J*-aggregates provide a high-density sample as compared to a single molecule, the fluorescence counts rate is therefore less sensitive to quenching. Furthermore, the rapid delocalization of energy away from the tip may serve to reduce the effect of a quenching process [10].

The largest *J*-aggregate bundles produce a far field background that is superimposed on the near-field signal [cf. Fig. 2(a)]. The near-field information is only a few percent of the total background. In regions of low aggregate concentrations, no far field fluorescence is expected, but the background counts are still high. The origin of this background can be revealed in the spectrum seen in Fig. 4. The spectrum represents the emission of the tip itself taken with the presence of the glass substrate. Fig. 4 was background corrected by acquiring a spectrum without the tip. Several features can be recognized. First, a sharp peak in the blue (390 nm) represents a second-harmonic generation. Second, a broadband continuum of light, starting in the visible and extending into the near infrared is also present. The origin of these two phenomena are revealed in the next sections.

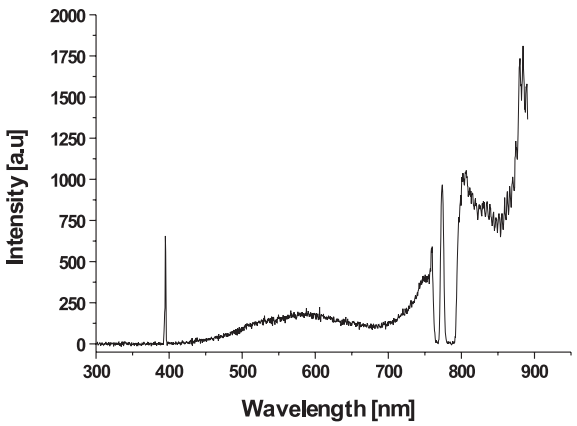

Fig. 4. Emission spectrum of gold tip excited at 780 nm by the longitudinal field in focused Gaussian laser spot on a glass cover slip. A second-harmonic peak situated at 390 nm and a broad band continuum is readily seen. The shape of the spectrum around 780 nm is due to the laser notch filter.

4. Localized second-harmonic source

Second-harmonic (SH) generation in gold has been extensively studied in the past. Many experiments investigated the nonlinear properties of thin films and their sensitivity to surface roughness [13]. The nonlinearity can be accounted for by a second-order nonlinear susceptibility of gold which gives rise to a surface nonlinear polarization at the second-harmonic frequency [14]. It has been shown that second-harmonic generation at a sharp gold tip can be modelled by a vertical on-axis oscillating dipole [15]. The surface morphology of the tip strongly influences the magnitude of the second-harmonic signal. Since the latter is directly excited by the enhanced field, one can expect an intense second-harmonic peak for a tip with a strong enhancement factor. We observed large intensity variations of second-harmonic generation from tip to tip. Unfortunately, we were not able to correlate the amplitude of the signal to any particular properties of the tip shape (as investigated by scanning electron microscopy).

Fig. 5 shows the distance dependence of the second harmonic signal as the tip is approached toward the glass surface. No significant difference in the SH dependence was observed between a tip approaching toward the surface or retracted from it. Similar to Fig. 3, the signal increases within the last 20 nm to the glass substrate. A single exponential decay can describe the second-harmonic tip–sample dependence. The decay length is on the order of the tip size (~ 30 nm), indicating that the second-harmonic signal is localized at the very apex of the tip. In consequence, the tip localizes an enhanced field at the fundamental frequency as well as at the second-harmonic frequency. The observed SH distance dependence is mainly governed by the decoupling of the SH evanescent fields at the tip from the substrate and the vertical variation of the longitudinal field strength which is strongest at the interface [9]. The approach curve of two-photon excited fluorescence in *J*-aggregates

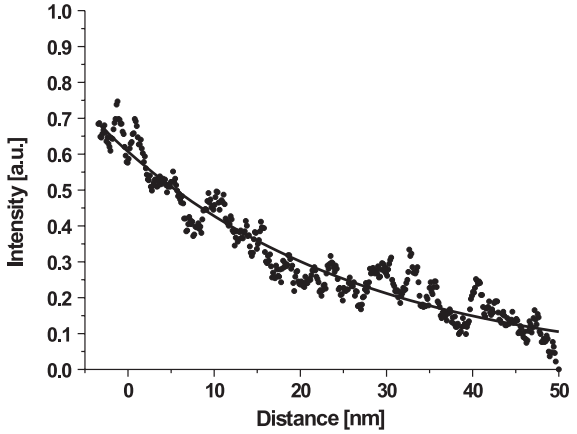

Fig. 5. Tip–sample distance dependence of the second-harmonic signal generated at a sharp gold tip. The experimental data (circles) can be fitted with a single exponential with a decay constant of 28 nm (solid curve).

of Fig. 3 is steeper than the approach curves for SH. The reason for this behavior is the fact that the source for fluorescence is the localized field at the tip, whereas the source for SH is the longitudinal field of the laser focus. Because the enhanced field is more localized than the longitudinal field of the laser beam, the approach curves are different for the two processes. Note that the tip used to measured the SH distance dependence is different from the one used to image *J*-aggregates, however, the measured SH decay length is reproducible between tips that have similar radii.

5. Confined broad-band continuum

As shown in Fig. 4, the second-harmonic peak is not the only spectral feature emitted by the tip. A broad-band continuum is also present. The continuum is relatively featureless, although the overall shape varies from tip to tip. Visible photoluminescence from metals was first reported by Mooradian [16]. Because the reported spectra did not depend on excitation wavelength, the origin of the emission was assigned to radiative recombination of holes in the *d*-band with electrons in the conduction band. More recently, local field enhancement due to surface plasmons has been found to be a prerequisite for efficient continuum generation [3], and local field enhancement in two-photon excited visible photoluminescence from rough metal films has been investigated [17]. Near-field studies of rough silver films showed that photoluminescence predominantly originates from a few locations (hot spots) where the presence of local plasmon modes leads to very large field enhancements [18,19].

Two phenomena have to be distinguished in the spectra of Fig. 4: visible emission on the blue side of the excitation, and infrared emission on the red side ($\lambda > 780$ nm). Our spectral measurements suggest that infrared photoluminescence is not the spectral tail of the visible photoluminescence but originates from a different mechanism. This difference is emphasized by the fact that the yields of visible and infrared photoluminescence do not have the same dependence on excitation intensity. As shown in Fig. 6(a), the visible emission intensity measured between 500 and 700 nm has a quadratic dependence on the average excitation power. This nonlinear behavior can be ascribed to a two-photon absorption process. As for the infrared part, it depends linearly on excitation intensity [cf. Fig. 6(b)]. We assign these infrared photons to transitions within the conduction band. Such transitions would not be expected since they involve states with large momentum separation that cannot be provided by a propagating photon [20]. However, as seen in the approach curve of Fig. 7, the photoluminescence has a distinct near-field origin. The experimental data can be fitted by an exponential decay with a characteristic length of 33 nm. The decay length is consistent with the size of the tip, and it is representative to the multiple measurement acquired with various tips. The distance dependence is governed by the same mechanism responsible for the SH distance dependence, i.e. evanescent wave decoupling and sensitivity to longitudinal field strength. We can conclude that the photoluminescence is also confined at the tip apex and momenta associated with near-field photons can therefore be much larger than momenta of free propagating photons. Direct transitions within the conduction band are

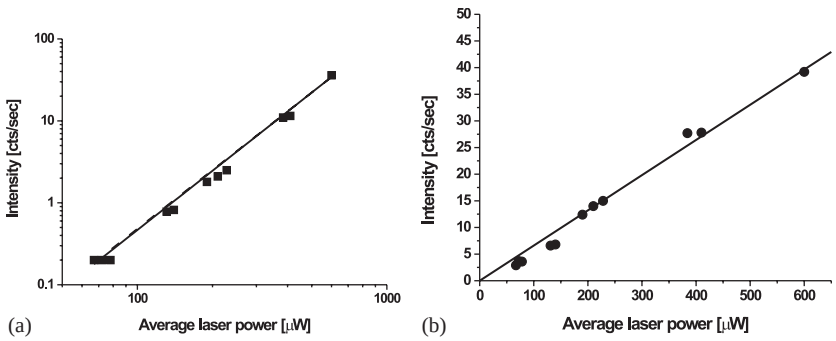

Fig. 6. Power dependence of the visible (a) and near infra-red (b) parts of the spectrum (Fig. 4). The visible depends quasi-quadratically on the average excitation power (slope 2.3, log–log scale) whereas the infra-red part increases linearly with excitation (slope 0.06).

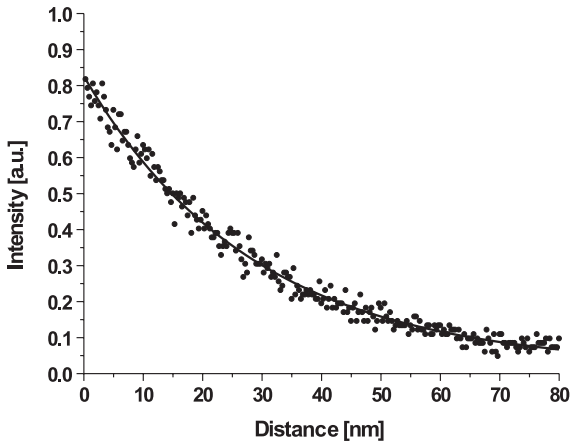

Fig. 7. Tip–sample distance dependence of the white-light continuum (500–700 nm) generated at the apex of a sharp metallic tip. The experimental data (squares) can be fitted with a single exponential with a decay length of 30 nm (solid curve).

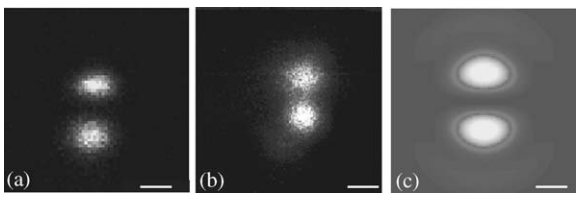

Fig. 8. Spatial distribution of second-harmonic (a) and photoluminescence (b) acquired with different tips. (c) Calculated distribution of longitudinal fields in the focus of a Gaussian beam (NA = 1.3). Scale bar: 250 nm.

now possible and give rise to the infrared part of the spectrum [21].

6. Confined light source as a probe for focal fields

Since both second-harmonic generation and photoluminescence result from the interplay between the localized enhanced field and the tip material, their responses must exhibit the same dependence on excitation polarization. To investigate the polarization sensitivity, a tip is laterally scanned through the focal region of a Gaussian beam. For each tip position, the intensity of the second-harmonic or the photoluminescence is recorded. Figs. 8(a) and (b) show that the two signals are confined to a two-lobe region. The calculation of Fig. 8(c) shows that the longitudinal field distribution in the focal plane of a focused Gaussian laser beam renders the same two-lobe pattern. Therefore, we can conclude that second-harmonic and photoluminescence are generated only when the tip is excited by longitudinal fields and an enhancement is created. The measurements were performed with two different tips, and the variation of the distance between the two lobes in Figs. 8 (a) and (b) originates from slight variations of the focus [9]. Since the two signals are sensitive to on-axis fields, the tip can be used to map out longitudinal fields. This is demonstrated here for a Gaussian beam, but the method can be extended to higher-order modes and configurations.

7. Conclusion

We demonstrated the use of longitudinal fields to excite an enhanced field at the apex of a sharp metallic tip. This enhanced field acts as a local light source for the excitation of fluorescence via a multi-photon absorption. Imaging of *J*-aggregates was demonstrated with a lateral resolution of 25 nm. We also showed that the tip responds to the field enhancement by generating second-harmonic signal and broadband photoluminescence. Tip–sample distance measurements demonstrate that these three phenomena, i.e. enhanced field, second-harmonic, and photoluminescence, are confined to the very apex of the tip. The polarization sensitivity of the tip's response can be used to map out the spatial distribution of longitudinal fields. Furthermore, it can be expected that the nanoscale second-harmonic and white-light sources can be employed to perform local absorption spectroscopy or in nanolithography.

Acknowledgements

The authors benefited from helpful discussions with A. Hartschuh and J.J. Greffet. The authors gratefully acknowledge the Swiss National Science Foundation (A. B.) and the NSF Grant No. DMR-0078939 for their financial support.

References

[1] K. Kneipp, Y. Wang, H. Kneipp, I. Itzkan, R.R. Dasary, M.S. Feld, Phys. Rev. Lett. 78 (1997) 1667.
[2] S. Nie, S.R. Emory, Science 275 (1997) 1102.
[3] J.C. Tsang, J.R. Kirtley, T.N. Theis, Solid State Commun. 35 (1980) 667.
[4] M.I. Stockman, Phys. Rev. Lett. 84 (2000) 1011.
[5] J. Wessel, J. Opt. Soc. Am. B 2 (1985) 1538.
[6] L. Novotny, R.X. Brian, X.S. Xie, Phys. Rev. Lett. 79 (1997) 645.
[7] L. Aigouy, A. Lahrech, S. Grésillon, H. Cory, A.C. Boccara, Opt. Lett. 24 (1999) 187.
[8] A.V. Bragas, O.E. Martínez, Opt. Lett. 25 (2000) 631.
[9] L. Novotny, E.J. Sànchez, X. Xie, Ultramicroscopy 71 (1998) 21.
[10] E.J. Sànchez, L. Novotny, X. Xie, Phys. Rev. Lett. 82 (1999) 4014.
[11] K. Karrai, D.R. Grober, Appl. Phys. Lett. 66 (1995) 1842.
[12] D.A. Higgins, P.F. Barbara, J. Phys. Chem. 99 (1995) 3.
[13] C.K. Chen, T.F. Heinz, D. Ricard, Y.R. Shen, Phys. Rev. B 27 (1983) 1965.
[14] P. Guyot-Sionnest, W. Chen, Y.R. Shen, Phys. Rev. B 33 (1986) 8254.
[15] A. Bouhelier, M. Beversluis, A. Hartshuh, L. Novotny, Phys. Rev. Lett. 90 (2003) 013903.
[16] A. Mooradian, Phys. Rev. Lett. 22 (1969) 185.
[17] G.T. Boyd, Z.H. Yu, Y.R. Shen, Phys. Rev. B 33 (1986) 7923.
[18] V.A. Markel, V.M. Shalaev, P. Zhang, W. Huynh, L. Tay, T.L. Haslett, M. Moskovits, Phys. Rev. B 59 (1999) 10903.
[19] C. Anceau, S. Brasselet, J. Zyss, P. Gadenne, Opt. Lett. 28 (2003) 713.
[20] O. Jepsen, D. Glötzel, A.R. Mackintosh, Phys. Rev. B 23 (1981) 2684.
[21] M.R. Beversluis, A. Bouhelier, L. Novotny, Phys. Rev. B 68 (2003) 115433.